Spatial prediction of landslide susceptibility using Frequency Ration (FR) and Shannon Entropy (SE) models: a case study from northern Rif, Morocco.

Abderrazzak Es-smairi (essmairi.a@gmail.com)
Abdelmalek Essaadi University Faculty of sciences Tetouan, Morocco
Brahim Elmoutchou
Abdelmalek Essaadi University Faculty of sciences Tetouan, Morocco
Riyaz Ahmad Mir
Geological Survey of India
Abdelouahed El Ouazani Touhami
Abdelmalek Essaadi University Faculty of Sciences, Tetouan, Morocco
Mustapha Namous
Sultan Moulay Slimane University Polydisciplinary Faculty of Beni Mellal

Research Article

Keywords: Northern Morocco, Tetouan-Bou_Ahmed, Landslides, Frequency Ratio (FR), Shannon Entropy (SE),prevention and assessment

Posted Date: March 23rd, 2022

DOI: https://doi.org/10.21203/rs.3.rs-1475332/v1

Abstract

In this study, a methodology for mapping and identifying the areas prone to landslides as well as to predict and reduce their impacts has been develop in the coastline between Tetouan-BouAhmed and its hinterlands, North Morocco. The area in the context of geological, morphological, climatic, seismic, and anthropogenic conditions is extremely favoring landslide occurrences. The trend of this phenomenon is expected to be growing over a course of time due to exceptional increasing rain events in response to climate change. A booming development of infrastructure and large quarrying activity, at the cost of forests on mountainous areas are strongly predisposed to mass movements. Their consequences are extremely large on various components such as on road network, habitat, hydraulic and electrical lines, protective structures, forest and vegetation systems, agricultural lands, littoral coast etc. For evaluating the susceptibility of landslide occurrences, the approach consists integrating a set of multisource data in GIS platform using Frequency Ration (FR) and Shannon Entropy (SE) models. For building these models, a total of 905 unstable slopes and eleven landslides causative factors were utilized based on multicollinearity test. Results of validation showed good prediction ability (> 76%) for both the models. However, the accuracy prediction indicated that the FR is about 3% more precise than SE model. More than 60% of the area is classified as dangerous that is prone to high landslide activities. The study may be of great importance to the managers and regulatory bodies for devising the guidelines for prevention, assessment, management and sustainable development in this region.

1. Introduction

Landslides of natural or anthropogenic origin in the northern Rif in Morocco and more precisely in the coastline area between Tetouan and Bou-Ahmed and its hinterlands are the most striking disasters in this region. This phenomenon ranked as a major “natural disasters” in many regions of the world (Glade and Crozier 2005; Zorn and Komac2007) is significantly growing up with the passage of time (Pradhan and lee 2010a) due to the heavy precipitation occurrences owing to climate change, continued deforestation, rapid increase in unplanned urbanization and development (Geotz et al. 2011). The frequency in landslides occurrences have become an extremely obvious reality and are considered responsible of dramatic damages and losses in infrastructure, in human life and economic development (Thieryet al.2007). The landslides includes all forms of displacement of slope forming materials/ or (Flageoll et al., 1989) that varies from debris flows to rock slides or combination of both. The combination effect of geological composition, landscapes complexity, abundant rainfall, seismic activity and the increasing magnitude of anthropogenic activities are considered the known framework of landslide conditioning factors at Rif scale (Millies-Lacroix1965; El Gharboui1980; Fares 1994;Es-smairi et al.2021). Similar factors are active at the coastline between Tetouan and Bou-Ahmed and its hinterlands in addition to the action of Mediterranean sea that continuously undermines in downstream mountains extending into the sea resulting in instabilityand slope failure (Es-smairi et al. 2021). The attracting geographical position of the coastlines and the hinterlands of the Rif domain, generally and more precisely covering our study area makes it more exposed to strong anthropogenic activitieslike the increasing housing and infrastructure

development. The construction of ports, hotels, golfs, marinas, roads networks, electrics lines, hydraulics etc., lead to the booming of large quarrying activities, deforestation over steep mountainous (Fig. 4f-i). To this is added the exceptional windstorms and torrential floods observed in recent years (e.g., 2000, 2009, 2013, 2015 and 2021)in the area. These, factor overall have undoubtedly exacerbate the vulnerability of this region to landsliding and its hazards. To supplement this, our field observations are also highlighting various landslides types (Fig. 3; Fig. 4) and thereby testifying an active morphogenesis (El Moutchou2014)in the area. The components most exposed to the landslides damages are road network, habitat, hydraulic and electrical lines, protective structures, forest and vegetation systems, agricultural lands, littoral coast (erosion and incision) and human life (Es-smairi et al.2021).

Thus, keeping in view, the intensity of the problem (Thiery et al 2007) it very imperative to to understand landslides process, determine the responsible and triggering factors and highlighted high risks areas for predicting, assessing, mitigating impacts and losses related to these Geohazards. For this reason, one of the main approaches more appropriate and conclusive is creating landslides susceptibility map (LSM) (Nohani et al 2019). Many methods and techniques have been developed for this purpose especially with the advent of GIS and remote sensing technology. Three main groups of techniques include the deterministic methods, qualitative methods and quantitative methods (Dai and Lee 2002). The deterministic methods are based on the calculation of safety factor by using mathematical relationship and physical law (Nohani et al 2019) and is considered is more appropriate for restricted areas. The qualitative methods, are contented essentially on the terrain characteristics and the expert knowledge (Van Westen2000), and therefore the results can be rather at highly subjective; geomorphological (Buwal1997 ; MATE/METL 1999). The qualitative indexed heuristic (AHP) (Yalcin et al 2011;Pourghasemiet al2012a;Pourghasemi et al.2013;Althuwaynee et al.2014;Brahim et al 2018;Es-smairiet al. 2021) methods are part of these group. The quantitative methods are the most experienced in landslides susceptibility mapping. These models are inspired from the basis of mathematical algorithms, statistical models (bivariate, multivariate, and combined models) by quantifying the relationship between landslide and causative factors. The most successful statistical models used in landslides susceptibility zoning are: Frequency Ratio (FR) (Pradhan 2010;Yalcin et al 2011; Pradhan and lee 2010b; Park et al. 2013;Iqbal et al 2021), Weights of Evidence (WoE) (Regmi et al 2010;Pradhan et al.2010a;Sadisun et al.2018;El moulat and Brahim2018;Iqbal et al 2021; Essmairi et al.2021), Analytic logistic regression (LR) (Pradhan and lee 2010b;Park et al. 2013;Rasyid et al. 2016, Wu et al.2017;Saha2020); Information Value (IV) (Karim et al.2019); Evidential Belief Function (EBF) (Nohani et al 2019), Fuzzy logic (Pradhan 2010,2011;Pourghasemi et al.2012a),and Shannon Entropy (SE) (Pourghasemi et al.2012b, Khosravi et al 2016,Nohani et al 2019), these groups of models cited allow to overcome the subjectivity linked to the opinion of the expert.Recently, machine learning and deep learning techniques are highly sought for geotechnical applications, landslides susceptibility risks and management (Zhang et al.2015), in term of example we can cite, neuro-fuzzy (Pradhan 2013), support vector machine (SVM) (Pradhan 2013;Van Den Eeckhaut et al.2012; Bui et al 2016,Saha2020), artificial neural network (ANN) (Pradhan et al.2010b; Pradhan and Lee 2010a; Pradhan and lee 2010b; Bui et al 2016,Saha2020), Random Forest (RF) (Li et al.2015; Saha 2020), convolution neural network (CNN) (Ghorbanzadeh et al.2019), decision three

(Pradhan 2013) and many others. The choice of one of these methods mentioned before in landslide susceptibility zoning and assessment is still a large topic for a debate (Guzzetti et al. 1999; Van Westen et al.2006).

The Rif areas of Morocco, is known for its spectaculars, frequency and variety of landslides. Millies-Lacroix (1965) is the first author who initiated inventorying and modelling landslides by applying heuristics method to produce a forecast risk map at 1 / 1.000.000 scale. Since then, respectable local studies were achieved using terrain characteristics and the expert knowledge for inventory and mapping landslides susceptibility (El Gharbaoui1980; Fares 1994; ElMoutchou2014; Brahim et al.2018, Es-smairi et al.2021). However, landslide susceptibility mapping and assessment using various bivariate and multivariate models is still less experienced at Morocco scale. Some few attempts to study landslides, like inventorying and susceptibility mapping assessment using statistical algorithms (bivariate and multivariate) using wofE, LR and other models are carried out by (El moulat and Brahim2018, Es-smairi et al.2021) (Brahim and El moulat2018).

Keeping in view, above facts, the main aim of this study is to identify and highlight the major factors in triggering landslides, and to explore the vulnerable zones which constitute a potential danger by using the Frequency Ratio (FR) and Shannon Entropy (SE) model. The guidelines for prevention, assessment, mitigation damages and for a good management will also be provided.Finally the prediction power of the two models using in landslide susceptibility zoning will also be assessed.

2. Study Area

The study area is located in the NW part of northernmost Morocco (Fig. 1). It is bordered to the East by the Mediterranean Sea, to the West, North and South by the dorsalecalcaireof internal Rif. The study area covers an area of 1478,428 km²and extends between the geographic coordinates of 35 ° 20’-35 ° 45’ North latitude and 5 ° 40’- 4 ° 40’ West longitude. From a geological, geomorphological, climatic and hydrographic point of view, the majority of this area is part of the internal Rif or Alborandomain. Geologically (Fig. 1b), the internal Rif or Alborandomain is grouped into three lithological units (Suter 1980) such as (1)the Sebtides of mantle and crustal origin more or less strongly metamorphic terrain; (2) the Ghomarides or Paleozoic nappes corresponding to the epi-metamorphic Schistous terrains inherited from the Variscan chain (El kadiri1991) and (3) the limestone ridge (dorsalecalcaire) corresponding to relics which has been the part of southern passive margin of the Tethys ocean (Chalouan et al 2008). It possesses a set of small nappes reinforced with Triasico-Liasic carbonates (Wildi1983). Besides this structural complexity (structuring in nappes of loadings), the very young character of the relief makes the region a very rugged mountainous area. In addition to the aforementioned internal domain, it should be noted that there are some extensions limiting the domain of flysch constituted by Cretaceous and Tertiary sediments, and the external domain represented by the Tangier unit. Geomorphologically, the study area is characterised by the succession of the high rugged countries with strong slopes (the croups of the Haouz, the ridges, the headlands, the cliffs) and low countries (the alluvium plains, the sandy coasts) (Fig. 3).

In the area, the climate is under the combined influence of the Mediterranean and the Atlantic type. However, the Mediterranean influence remains predominant. A hot and dry summer, and a wet and mild winter is witnessed. It varies with latitude, altitude, influence of sea, desert, continentally, NE trade wind, Canary currents, slope aspect and monthly seasonal changes and diurnal (Thauvin1971; El Gharbaoui1987). The average annual rainfall can reach 654mm.Hydrographically the internal Rif consist of permanent or temporary rivers with irregular flow regime. They are largely encased with great meanders in the northern part, and narrow encased and perpendicular to the coast in the meridional part. The geographical position of the Rif domain, on the borders of the African and Eurasian plates, makes the area an active seismic zone with a moderate intensity under the effect of Alboran and Acores which are reported very active seismic zones. Thus, all these characteristics cited before make this areas a hot spot to landslides occurrence.

3. Materials And Methods

In the present study, workflow of methodology followed is given in Fig. 2. The methodology is based on satellite, geological, topographic, and meteorological data sources, in addition to observations collected during the field survey and investigation. The data were further analysed and integrated in GIS platform. Accordingly the FR and SE models were used to generate elaborative landslide susceptibility maps. For the purpose of assessment and validation of landslide susceptibility maps, the (AUC / ROC) method were used. The details of the methods are given as

- In this study, the ASTER image (GDEM) (Advanced Space borne Thermal Emission and Reflection Radiometer, Global Digital Elevation Model) was used. The ASTER image in Geo TIFF format, with a resolution of 30 meters is distributed for free download through the USGS Earth Explorer Community site (http: //earthexplorer.usgs.gov/). The image scene (id: ASTGTM2_N34W005, ASTGTM2_N34W006, ASTGTM2_N35W005, ASTGTM2_N35W006), were acquired on March 15 2011 was used in this study.
- A Landsat 8 satellite image acquired on 2017-09-14 also used. This data image was available for free download on the USGS Earth Explorer Community site (http://earthexplorer.usgs.gov/);
- Geological maps at a scale of 1/50 000 of the region of TetouanRasMasari, Talamboute, Bou Ahmed, and part of Beni Hassan was also used. The whole data was geo-positioned according to the Lambert conformal conical projection of the northern zone of Morocco.
- Topographic maps of Tetouan, RasMazari, Talembote, Bou Ahmed, and part of BeniHessane at the scale of 1/ 50.000; positioned according to the Lambert conformal conical projection of the northern zone of Morocco were also used;
- Aerial photographs of the 1958 and 1986 missions of the Mediterranean coastal fringe between M’diq and OuedLaou were also acquired and used.;
- Average annual rainfall from 1970 to 2017 of stations located in our study area and those neighbouring was acquired and used;from the Watershed Agency of Loukkos (ABHL) Tetouan Morocco.

- Additional data collected from terrain during several monitoring fields missions was also used. The inventories of landslides and direct investigations in the terrain (slope break zone, dip, cracks, fracturing, schistosity, faults, escarpments, ridges, crevices, replats etc.), was also collected. The field survey was carried during rainy season and the dry season from 2014 to 2020 at around forty well-distributed sites spread throughout the study area.

3.1. Landslide mapping and inventorying

In this study, the field survey has been carried out from October 2014, for mapping landslides events using the GPS. The field survey was coupled with extracted data from, topographic maps, geological maps, satellite images (Landsat-8) and aerial photographs/data. This step was of great importance on the one hand in building the landslide inventory map for our study area and on the other hand to evaluate the correlations between the landslide's causative factors and the spatial distribution of landslides. A total of 905 unstable spots covering an area of 95,838 km² were identified. These unstable spots correspond to 6,482% of the total of the study area. Thereafter, the landslides inventoried were randomly divided into two groups; that is 1) landslide training data consisting about 78% from the total of inventoried landslides. This training data was used to build the model and 2) the remaining data of landslides which consists about 22% was used for validation purpose of the model performance. This data set is therefore also called testing data (Fig. 3). In the study area, numerous types of landslides were identified and mapped such as surface gullying (Fig. 4d), earth flow (Fig. 4a), complex slides (Fig. 4i), rotational slides (Fig. 4e), transitional slides (Fig. 4b), debris flow ((Fig. 4c), rocks falls and mass detachment etc (Fig. 4f).

3.2. Causative factors of landslides

Landslides occurrence process is complex and dynamic. It varies from place to place which makes their comprehension very difficult and therefore, it is very imperative to unify them by a single model to understand and assess. Generally, the landslide initiation and occurrence is a combined result of a number of causative geo-factors factors that are either natural or anthropogenic (Varnes1978; Crozier 1984). In the current study and based on field surveys, literature, effectiveness, and availability of data, eleven factors were selected to analysis the occurrence, spatial distribution of landslides and to produce landslides susceptibility maps. These factors were the elevation, slope, aspect, curvature, hill/shaded, proximity to streams, proximity to faults, proximity to roads, land use, lithology, and rainfall. The topographic factors (elevation, slope, aspect, curvature and shaded/relief) (Fig. 5a-e), the mps were generated from GDEM data. In addition, this image also was used for extraction of the major and main hydrographic/drainage network for preparing proximity to stream map (Fig. 5f). Furthermore, proximity to roads and land use maps (Fig. 5.g.h) were generated from topographic maps supplemented with Landsat image. The delineation through the process of digitization of all lithological units and structural lineaments (faults, thrust) from geological maps, allowed to prepare a detailed lithological map and proximity to faults map (Fig. 5i,j). The annual rainfall data (1970 to 2017) from the watershed agency of Loukkos (ABHL) Tetouan Moroccohad been employed for the production of the rainfall distribution map

using IDW interpolation method (Fig. 5k). The close relationship between these factors and landslides occurrence is widely discussed and proved previously. The elevation exerts a great impact (linear relationship) on other factors such as slope, aspect, precipitation, gravitational force, water velocity erosion force and consequently influences strongly the landslides trigging. In this study, the elevation map subdivided into four classes (<25m; 25m-100m; 100-600m; > 600m) (Fig. 5a) (Essmairi et al 2021). Slope angle is also considered more important in landsliding (Van Den Eeckhaut et al. 2006; Hadji et al. 2013, Iqbal et al 2021) and it is observed that the shear forces increase with increasing slope angle. The higher slope angle lead to instability, triggering and become more important factor to impact the lithology with variable degree of cohesion and of weathering, and structural characteristics (faults, schistosity, fractures, diaclases). The slope map produced was classified into five classes: > 2.5; 2.5-5; 5-15; 15-20; <20 (Fig. 5b).

Landslides tend to occur in specific directions in certain places (Saadatkhah et al 2015). It is because, the orientation of slopes aspect affect the variations in humidity of the hillslopes (Ercanoglu and Gokceoglu2002), flow evapotranspiration and soil moisture (He et al. 2019; Jaafari et al. 2019) and the percentage of solar radiation in days (Iqbal et al 2021). In this study four classes of slope aspect were determined: The North slopes (315 ° -45 °); the western slopes (45 ° -135 °); the eastern slopes (135 ° -225 °) and the southern slopes (225 ° -315 °) (Fig. 5c). The curvature characterizes the morphology of terrain topography (Pourghasemi et al. 2013). The curvature map produced is classified into three classes: <-0.002 (concave topography); -0.002-0.004 (flat topography); <0.004 (convex topography) in this study (Fig. 5d). Since, the topographicforms have a contrasted role in surface drainage of rainfall water and thus, have a contrasted impact in landslides occurrence. The shaded relief map have been generated and was classified into 5 classes (0m-50m; 50m-100m; 100m-150m; 150m-200m; 200m-254m), (Fig. 5e). The relief is considered as an important morphometric element in morphological studies of landslides (Thapa and Bhandari2019, Iqbal et al 2021, Essmairi et al 2021). The relief influences other factors such as vegetal cover, water velocity and soil erosion (Vijith et al 2014) which in turn control landslides occurrence. Under the current study area, several instable spots have been located near the riverbanks, related to the concentration of erosion and the undermining near banks of river (Popescu1994; Pham et al. 2018). Keeping this situation in view, in this study, we use proximity to streams in modelling. This factor is therefore, classified into 10 classes as per proximity to streams (<30; 30-60; 60-90; 90-120; 120-150; 150-180; 180-210; 210-240; 240-270;> 270) (Fig. 5f). Proximity to Faults is also considered as an important factor in landsliding occurrence. The discontinuities created in soils and bed rocks (Ayalew et al. 2005), make them less cohesive and less resistant (Devkota et al. 2013) as well as favouring circulation and infiltration of water which is an agent of instability. The proximity fault map comprises 10 classes (<30; 30-60; 60-90; 90-120; 120-150; 150-180; 180-210; 210-300; 300-500;> 500) (Fig. 5g). The structural discontinuities were generated by digitalization of structural lineaments from the geological maps of TetouanRasMasari, Talamboute, Bou Ahmed, and part of Beni Hassan.

It is important to mention that the observations during field surveys also highlighted the impact of manmade activities (installation of roads, quarrying activities) in the activation and reactivation of spectacular instability spots. It is also observed that the rehabilitation in such area in future is difficult. To

assess the impact of anthropogenic factors in this study we use proximity to roads map were produced by digitizing the essentials of the national and regional road network based on topographic maps and the landsat-8 satellite image, these maps were divided into, 10 classes: <40m; 40-80m; 80-120m; 120-160m; 160-200m; 200-240m; 240-280m; 280-320; 320-360; > 360 (Fig. 5h). Beside this, demographic expansion and the development that has occurred in the study area in recent years, has also influence on the repercussion of instability of hill slopes. During this process, more areas of mountain and forest is utilized for urbanisation, overgrazing, agriculture lands, exploitation of quarrying….etc. At certain locationsit is accompanied without appropriate management which increase the susceptibility to hillslopes to landsliding and instability. Thus the importance of land use map in landslides occurrence is very high. In this study six land use classes have been identified such as water Bodies; barren land, sparsely vegetated, agriculture land, Settlement area; wood and forest (Fig. 4i).The land use maps are prepared and extracted using the digitalization of topographic maps (Tetouan, RasMazari, Talembote, Bou Ahmed, and part of BeniHessane) coupled with the supervised classification of the landsat-8 satellite imagery, using the maximum likelihood method.

Additionally, the lithology characteristics (geotechnical and geo-mechanical properties) re closely related to the landslides trigging in the study area in combination with other factors mentioned above as well as rainfall. According to the geotechnical and geomorphological affinities, 12 lithological classes were determined in the area. These include the Gneiss and Micaschists, Peridotites and Kinzigites, Shale complex, marlstones, Limestone, Dolomites, Sandstone-Pelite, Conglomerates, Sandstones-marlstones, Marlstones-limestone, limestones-dolomites and Alluvium (Fig. 5j).The abundance of rainfall is a very crucial factor in the occurrence of landslides in the study area. To highlight the spatial variations of the pluviometry; annual average rainfall (1970 to 2017) from the watershed agency of Loukkos (ABHL) Tetouan Morocco,has been used. The rainfall map have been divided into ,10 classes (> 500mm; 500mm-550mm; 550mm-600mm; 600mm-650mm; 650mm-700mm; 700mm-750mm; 750mm-800mm; 800mm -850mm; 850mm-900mm;> 900mm) (Fig. 5k) using interpolation method.

3.3. Landslides susceptibility modelling

3.3.1. Frequency Ratio (FR)

FR is a bivariate model, widely applied in several studies in various region of different context, to evaluate the susceptibility to landslides. It expresses the possibility of occurrence or not, of landslide, in a determined class of each factor, and therefore the evaluation of the relative importance of each factor is involved. Then, for each class of causative factor, the frequency ratio is obtained by simple dividing the landslide's occurrence ratio with the ratio of each class of this factor (Lee and Talib2005), according to equation (1). When, Fr <1, the correlation is weak between the occurrence of landslides and the weight of the factor class and vice versa (Pradhan 2013). The Landslides susceptibility index (LSI) can thus be calculated by summing the frequency ratios of all factors considered according to equation (2).

$$fr = \frac{N_i^p / N}{A_i^p / A}$$

1

$$\mathrm{LSI} = \sum_{\mathrm{j}=1}^{\mathrm{j}=\mathrm{n}} \mathrm{FRj}$$

2

(Where, N_i^p number of landslides pixels in classi of factor p, N number of landslides pixels in the total area, A_i^p number of pixels within class iof factor p, A is the number of total pixels of the study area)

3.3.2. Shannon entropy (SE)

The second model used in the present study is the bivariate index of entropy model. Pourghasemiet al (2012b) defined entropy as the measure of the degree of disorganization, unpredictability, abnormality or instability of the information content of a system. In this model, t the difference between the averages of the contributions of a single element in the entire system, called the entropy index is estimated (Wan 2009). Shannon entropy model is characterised by an extreme relationship between the quantity and entropy, named Boltzmann, which is utilized to show the thermodynamic conditions of a system (Pourghasemiet al 2012b). SE can identify most controlled and influencing factor of the landslide occurrence from a several causative factors used,. The following equations were used to calculate the information of coefficient:

$$E_{ij} = \frac{FR}{\sum_{j=1}^{M_j} FR}$$

3

Where FR represents the value of the frequency ratio and $E_{ij}$is the probability density for each class:

$$H_j = -\sum_{i=1}^{M_j} E_{ij} log_2 E_{ij}, j = 1, \ldots, n$$

4

$$H_{jmax} = log_2 M_j, M_{j-EquationNumberofclasses}$$

5

$$I_j = \left(H_{jmax} - {H_j}/{H_{jmax}}\right), I = (0,1), j = 1, \ldots (6)$$

6

$$V_j = I_j FR$$

7

Where H_j and H_{jmax} are the values of the antropy, I_j is information coeffcient, M_j is number of classes in each conditioning factor, and V_j is the achieved weight value for the given parameter. The result varied between 0 and 1. The values close to 1 indicate a higher instability (Khosravi et al 2016).

4. Result

4.1. Multi-collinearity diagnosis

To ensure the independence between all factors, a multi-colinearity test was carried out by the variance inflation factors (VIF) and the tolerance method. According to Pourghasemiet al.2012b, when the tolerance <0.1 or VIF> 10 is worth identifying a problem in the multicollinearity between the selected factors. In this study, the results of the test as given in (Table.1) show that the smallest value of tolerance is 1.009, and the largest value of VIF is 5.141. It thus indicates that there is no-multicollinearity observed for the eleven factors chosen in this study. This finding is highly identical with Es-smairiet al. (2021).

4.2. Application of Frequency Ratio (FR)

In this study, the application of the FR model allowed to highlight the relationship between the landslides occurrence and each class of analysed causative factors (Table .2). The value of the FR determines the correlation weight between factors and landslides occurrence. A value of FR greater than 1 affirms a strong impact in triggering landslides and vice versa (Pradhan 2011). While analysing the elevation impact, the most susceptible class exposed to the instability of the hill slope altitude ranges falling between 100m-600m with a FR = 1.253. The most stable area against occurrence of landslides lies between an altitude zones of 0m-25m. Concerning slopes, the classes which have more impact on the instability of the hill slopes include the classes of 5 °-15 ° (FR = 1.353) and 15 °-20 ° (FR = 1.110) respectively. The slopes classes less than 5° are the most stable to landsliding in the area. The influence of the slope direction (aspect) indicates the North facing slopes with FR=1.137 being slightly dominant in the triggering landslides. It is followed by the West facing slopes (FR=1.077) and the East facing (FR=1.004) respectively. Regarding the curvature factor, the concave hill slopes have a very important impact on landslides occurrence (FR=1.101). The hill-shaded factor, which varies between 0m and 254m, shows a positive correlation between relative relief and the occurrence of landslides. The class “200m-254m” shows the highest correlation with the Landslides. A perfect correlation between the genesis of the occurrence of landslides and proximity to rivers is noted in the area. For instance, the closer we get to streams the more impact is influenced. At this crucial zone, the erosion by undermining is intense. The areas which constitute places favourable to the initiation and evolution f landslides are, the zone located at a distance of <30m (1,294) on both sides of the rivers, followed by the zone which includes between 30m-60m (FR = 1.245), and the area between 60m-90m (FR = 1.134).

Geologically, the areas close to the structural lineaments (faults, fractures, lithological contact), remain potential areas for the origin of the landslides as a result of its mechanical weakness (fractured, brecciated zone) and their power of diffusion and transmission of water. In this area, with the exception of the first two and the last class, all other classes show significant influence on the susceptibility of occurrence of landslides. The area between 150m and 180m on either side of the lineaments constitute a favourable place to initiate and develop mass movements (FR = 1.497). To assess the impact of anthropogenic action in our study, we took the example of the establishment and development of the roads network, which requires excavation, drilling, percussion by machines and sometimes use of explosives and overweight or void creations by earthworks or supports. These actions are more than enough to activate or reactivate the process of triggering mass movements on a hill slopes that are otherwise, naturally stable (i.e. national road N16). The areas that are more susceptible to landslides are those located near the road and as we move further away the risk decreases. However, the analysis of frequency ratio of classes of roads shows a negative and weak correlation in landslide trigging near roads sides. In the case of land use impact, bare land is the most exposed to landslides (FR=1.094). Another factors most involved in mass movement trigging is lithology, it can be seen that the lithological units such as, Sandstones-marlstones, Marlstones-limestones, Sandstones-Pelites, Conglomerates, Limestones-dolomites, Limestones and Dolomites, contains the highest value of Frequency ratio (FR=2.864; FR=2.517; FR=1.287; FR=1.801; FR=1.216; FR=1.095; FR=1.089), thereby, indicating a very high correlation with initiation and occurrence of landslides. The other units (Gneiss and Micashists, Peridotites and Kinzigites, Shale complex and Alluvium) have low correlation (FR<1) as given in (Table .2). In addition to the lithological factor, and the geomorphological conditions, the abundant rainfall in the area also participate in the surface gullying and the bursting of the rock soils due to water saturation, thereby reducing the cohesion and resistance of the hill slopes. In our study area, a positive correlation between rainfall and spatial distribution of landslides is observed, except for the last three classes that represent the highest rainfall in the area but a weak occurrence of landslides (FR<1) (Table .2)

The landslides susceptibility map (LSM) was generated (Fig. 5a) by assigning the weight of FR obtained for each class of the above factors.The weight of FR were then added according to the following Eq (8):

$$LSM_{FR} = FR_{Elevation} + FR_{slope} + FR_{Rainfall} + FR_{Lithologuy} + FR_{Landuse} + FR_{Shaded/relief} + FR_{Proximity\ to\ streams} + FR_{EleProximity\ to\ faults} + FR_{Aspect} + FR_{ElevCurvature} + FR_{Proximity\ to\ roads} \quad (8)$$

4.3. Shannon Entropy (SE) model

According to the results obtained (Table.2), the parameters which influence the instability of hill slopes and therefore the triggering of landslides in decreasing order of their weights and susceptibility are, rainfall, altitude, slope, lithology, proximity to streams, land use/cover, proximity to lineaments, shaded relief, aspect, proximity to road network and curvature. This succession of the weight impact of causal factors is perfectly logic and can be correlated with our knowledge of the study area and other

characteristic. The combination of the weights of these factors according to Eq (9), allows us to obtain the landslide susceptibility map (LSM) (Fig. 6b).

$$LSM_{SE} = \quad 0{,}238 * \text{Rainfall} + 0.200 * Elevation + 0.175 * Slope + 0.141 * lithology + 0.074 * Proximity\ to\ streams + 0.065 * Landuse + 0.053 * Proximity\ to\ faults + 0.028 * (Shaded/relief) + 0.016 Aspect + 0.004 (Proximity\ to\ Roads + 0.005 Curvature \quad (9)$$

Finally, two landslides susceptibility maps (LSM) maps were generated according to the FR and SE models (Fig. 5). The generated maps are reclassified into five vulnerability classes such as Very low, Low, Moderate, High and Very high using natural break method. The analyses of the results (Fig. 5a,b andFig.6) shows that for FR model, Very low, low, moderate, high, very high covered 9.405, 5.407, 24.415, 38.739 and 22.032% of the study area r. For SE model, with almost some percentage as calculated in the model FR, 9.368, 5.454, 23.434, 39,978 and 21.764% were covered respectively, corresponding to the classes Very low, low, moderate, high and very high.

5. Discussion

5.1. Causative factors analysis

During recent years, the application of statistical bivariate models (i.e. FR, SE, WofE, EBF, LR, IV…etc.) to create landslides susceptibility maps (LSM) have become one of the compelling methods and are thus, widely used for landslides hazard assessment, mitigation risks and good management of territories (Guzzetti 2006; Pham et al.2018). Likely, in the current study area and its surroundings, several models have been tested effectively in numerous studies. The previous studies so far not suggested in favor of any one model better than another (Guzzetti et al. 1999; Van Westen et al.2006). The variable and better results are always attributable to the structures of the models used and the quality of the input data (Pham et al. 2018).

The process and the spatial distribution of landslides, generally cannot be understood and explained by a single factor, but is attributed to a combination of more than one factor (Varnes1978; Crozier 1984). Therefore to have better understanding and quantifying the relationship between the landslides occurrence and the eleven causative factors (i.e. altitude, slope, aspect, curvature, shaded relief, proximity to streams, proximity to lineaments, proximity to road network, land use/cover, lithology and rainfall), and to determine the important causative factors, the current study has been carried out... This study and the steps involved are very crucial for better guiding, and promoting the prevention plans against landslides incidences by targeting the predominant factors. Thus, in this study based on Shannon entropy modeling in the region of Tetouan-Bou Ahmed and its hinterland, northernmost of Morocco, it was found that rainfall followed by elevation, slope and lithology are the most effective factors in landslides trigging. This finding is consistent with our field observations and others studies carried out in the Rif area (Millies-Lacroix1965; Fares 1994 ; Al Gharbaoui1980; Chaouni1999 ;El Kharim2002 ; Moutchou2014; Brahim et al.2018; El moulat and Barhim2018). The other factors such as proximity to stream, landuse, proximity to faults, shaded relief, aspect, proximity to roads and curvature are respectively less involved in landslides

occurrence in the area. A quantitative comparison of the results between models, it is found suitable to use this dataset in building these models (Iqbal 2020). Es-smairi et al. (2021), using AHP and WofEmethods, found approximately similar result; in thisregion for building models with a main difference of priority rankings of major and secondary causative factors in landslides occurrence. As mentioned before, having an idea of the weight of the impact of the factor in the triggering of mass movements represents a very important step in the studies of prevention and mitigation of risks. This could still perform by giving more details on the vulnerable areas exposed to the action of a given factor. For this purpose, we were used FR model for highlighting the critical areas to landsliding. The analyses of FR results showed that, as expected, a linear correlation between elevation and landslidingis found. This correlation further showed that the more we advance towards the high countries (JbelKelti,JbelEfrane,HafatJeltane, JbelTazout,Jbeldarsa), the frequency of terrain instabilities increases. However, a decrease in frequency is observed in the high ridges of the limestone and dolomite due to its resistance against water erosion and weathering processes. In addition, the area has abundant cover of vegetation and forest, which helps in stabilization of the hill slopes (Es-smairi al al. 2021).

The moderate elevations (100-600m) is the most vulnerable to slope failure under study area. It is because; these elevations overlap with Ghomarides nappes, the Sebtides, flysch nappes and the tangier units, which are very predisposed to landsliding. It is due to occurrence of predominantly of flyschs deposits that are very deformed, altered and poorly resistant. The very low and low elevation area, which superpose with flat areas corresponding to the furrows of the main rivers, the alluvio-marine and plains, and the sandy coasts are the most stable areas to landslide occurrences. The same is observed for slope factors that is the susceptibility to landslide risk increases as the slope angle is increasing., We note that the linear correlation of slope and landslide occurrences in the area is interrupted for two last classes which can be however, explained by the superposition of these slopes at the crests and cliff of Calcareous Dorsaland sandstone bars that are rheologically competent and resistant. Similarly, the north direction aspect followed by West and East aspect had the most impact on landsliding process respectively. These directions are less exposed to solar radiation and more wetness as observed is due to the wet currents of the Mediterranean Sea and the Atlantic Ocean, whereas south-facing hill slopes more exposed to solar radiation show a weak impacton slope movements. Among the curvature classes, the concave hillslope class has the greatest probability for slope failure. It is probably due to the capacity of these topographic forms to collect rainwater that after percolation leads to leaching and alterations of the rocky material and consequently the reduction of the mechanical resistance of these slopes (Es-smairiet al.2021). Further, the results of proximity to streams showed that it closely exerted an important impact to undermining of the base of hillslopes, especially after intense rainfall. The debris flow and sliding are common under study area. The disconnection in soil and rocks related to the faults and the major contact between geological formations constituting an important conduit for water circulation, which are the main causes responsible for landslide trigging. Under study area, many water sources flow along its geological contacts constituting sources of drinking water supply for several villages (i.e. source of Bni Salah, source of BeniHarchan, source of Bouaanan, source of Ezzarka etc.), In this study, the results show that the distance between 90 and 500m from fault constitute the areas more prone to landsliding. Our

field observation show that, in addition to the impact of the proximity to the sea (undermining of the continental shelf by dynamic and erosion of water sea) the installation of the coast national route 16 (N16) that connects Tangier on the northwest coast of Morocco to Saïdia on the northeast coast passing through study area, was the major cause of the local activation and reactivation of some hot spot landslide occurrences, .However, the results show a weak relation between landslides occurrence and proximity to roads this probably is due to the moderate number of landslides mapping along roadside and a large part of roads network pass under flat zones.

In term of landuse and as expected, the barren lands deprived of cover vegetal are more exposed to water erosion and sliding. Lithology is one of the most determining factors in the occurrence of landsliding in Rif domain; since this factor has undergone a very intense tectonic stresses (e.g., shear zones, foliation, fractures, faults, folds). The presence of a very contrasted climate with very intense rainy periods, these processes accentuate the alteration process of lithology (dissolution, karstification, disintegration, soil formation etc) that lead to mass wasting and weakens their cohesion and resistance to landsliding and erosion .Among the lithological units that show a very strong susceptibility to mass movements are sandstones-marlstones and marlstones-limestones respectively., These later overall are calcareous clays moderately plastic and with a weak mechanical strength. Besides this, the annual rainfall factor is relevant in landslides trigging especially after heavy rainy days. The water saturation decreases the cohesion forces and the shear strength which gives rise to triggering instabilities (Song et al. 2012; Hamed et al. 2014). The results show a linear relationship between rainfalls and spatial distribution of landslides except for the last three classes that show a less influence in landsliding process. This disagreement is probably due to the fact that these classes superpose with high elevation that are constituted by limestone and dolomite of calcareous dorsal that are less sensitive to landslides and water erosion. These results of FR model are in agreement with results of WofE model using by Es-smairi et al (2021).

Overall, in light of these results obtained from FR and SE model generally, we can note that on the one hand, the models function almost similarly; on the other hand, the most important factors of instability of the hill slope and consequently on landslides occurrences are elevation, rainfall, slope and lithology. The analyses of the maps as shown in (Fig. 6a,b) and the results of (Fig. 7a,b), it is found to be highly in agreement with the terrain condition reality and the spatial distribution of landslides in the area. Furthermore, approximately 14% of the study area does not constitute a real risk by landslides occurrences as it corresponds to flat zones (alluvium plains and sandy coasts). The area that is classified as moderately susceptible to slopes failure is represented by 24% of the study area. It coincides with high altitudes of the calcareous dorsal resists to erosion and weathering. But, this area, still and always represents a tendency towards collapse (rocks falls, debris slide) following the intense fracturing especially as a result of anthropogenic intervention (e.g., quarrying activity). Besides this, large area (60%) is classified as most dangerous zone that is highly exposed to landsliding. This area extends over the outcrops of the Ghomarides nappes, the Sebtides, the Flyschs nappes and the tangier unit, crossed by several river notches. These areas have undergone a very intense and complex kinematic course along its formation, recognised by significant metamorphism (e.g., folds, foliations schistosity, fracture, Faults

etc). It is accompanied with a strong supergene weathering area that makes them very fragile to instability. Just a tiny unearthing of the foot of a hillslopes, is enough to initiate the triggering process of landsliding. In summary, these results with quantitative methods, allowed to highlight the important and the close relationship between geological, geomorphological, hydrogeological, climatic and anthropogenic activities in the context of landslide occurrence in the coastlines between Tetouan- Bou Ahmed and its hinterlands.

5.2. Validation and comparison

Among the most crucial steps in any risk prediction modelling is the validation of the results obtained. The reliability of the results is also closely dependent on the quality of the data and the model used (Phamet al. 2018). In this study, verification and validation were done on the one hand, by a direct confrontation with the reality on the terrain (the inventoried instabilities), and on the other hand, by using the AUC curves of the ROC method (Yilmaz 2010). The ROC curve plots in the Y-axis shows the rank of the landslide susceptibility index in descending order whereas; the X-axis shows the cumulative percent of landslide occurrence corresponding to success and prediction rate, respectively (Trigila et al. 2015). A curve of a model with a largest AUC, which varies from 50–100%, can be considered the best model (Hong et al2018). The Analysis of the AUC results of the current study, shows that for the FR Model, the success rate using training data was 79.023% and for the prediction rate using validation data was 78.974%, (Fig. 8a,b).Whereas, for SE model, the success rate, and prediction rate were 76.689% and 76.016% respectively (Fig. 8a,b). It appears that FR model is very interesting for exploring areas prone to slopes failure compared to the SE model. In another study, carried by Es-smairi et al. (2021) using WofE and AHP, it was found that the prediction accuracy for both models is 74,653% and 71,394%, respectively. We can depict from this comparison that the prediction precision given by both models (FR and SE), is reasonable and consistent in term of production of landslide susceptibility maps under our study area, with clear advantage of FR model. This finding of accuracy and precision of FR modelling landslides susceptibility mapping is similar and appreciated with many studies in several regions of different context suffered by landslides occurrence, e.g., India (Kannan et al. 2013), Himalaya (Regmi etl.2014), Malaysia (Lee and Pradhan 2007), Indonesia(Rasyid et al.2016), Nepal (Thapa and Bhandari2019), Iran (Nohani et al. 2019), Turkey (Yalmiz2009), Algeria (Karim et al. 2019)and other context.

6. Conclusion

In this study, the mapping of landslide prone area has been carried out in the coastline between Tetouan-BouAhmed and its hinterlands northern parts of North Morocco. The methodology adopted in this work, proves the importance of the GIS environment, remote sensing, and the potentialities of the FR and SE models for landslides susceptibility mapping to elaborately better explain the conditions of hills slope instability.. Eleven trigger factors were selected namely, rainfall, altitude, slope, aspect, Shaded relief, curvature, lithology, proximity to the streams, land use/cover and the proximity of lineaments and integrated into GIS platform,. Two landslides susceptibility index maps were produced, and reclassified into five classes (very low, low, moderate, high, very high). Subsequently, the maps were verified and

validated by comparing with the inventoried landslides, and by using the ROC / AUC methods. The validation results obtained are conclusive and very satisfactory in terms of zoning of landslides risks in the study area. It should be noted that more than 60% of the total surface of study area, is unstable and is exposed to impact of landslides. Itis considered alarming and disturbing, especially with, the rapid proliferation of urban unplanned developmental activities. Nevertheless, the development of new tourist parks at the cost of deforestation of hills' slopes, and underestimating the impact of changing climatic conditions, especially with torrential rainfall, are considered to be the primary factor in triggering of landslides in the area. Therefore, to minimise the risk of landslides, it is recommended, to impose a large study of scenario protections medium and long term against the instability of hills slopes, to sensitize the population to the repercussions of deforestation, reforestation of barren land, and banning of agricultural practices on slope (>15°) prior to any planning of developmental activity. Moreover, understanding the processes of hill slope instability, and other triggering factors such as seismicity and the groundwater potential zone is also considered. Nevertheless, the landslides susceptibility maps produced, could constitute a basic document in the first phase of a planned development in the area.

Declarations

Acknowledgements:

We would like to thank and express our gratitude to the anonymous reviewers for their comments and suggestions.

Ethical statements and declarations

The authors declare that:

1. The article is original.

2. The article has been written by the stated authors who are all aware of its content and approve its submission.

3. The article has not been published previously

4. The article is not under consideration for publication elsewhere

5. No conflict of interest exists.

6. If accepted, the article will not be published elsewhere in the same form, in any language.

References

1. Althuwaynee OF. Pradhan B, Park HJ, Lee JH (2014) A novel ensemble bivariate statistical evidential belief function with knowledge-based analytical hierarchy process and multivariate statistical

logistic regression for landslide susceptibility mapping. Catena 114:21–36

2. AyalewL,Yamagishi H (2005) The application of GIS-based logistic regression for landslide susceptibility mapping in the Kakuda-Yahiko Mountains, Central Japan. Geomorphology 65(1-2):15–31
3. Brahim LA, Bousta M, Jemmah IA, El Hamdouni I, ElMahsani A, Abdelouafi A, Lallout I (2018) Landslide susceptibility mapping using AHP method and GIS in the peninsula of Tangier (Rif-northern morocco). In Matec Web of Conferences (Vol. 149, p. 02084).EDP Sciences
4. Brahim LA, Elmoulat M (2018) Application Of Logistic Regression Method To Produce Landslide Susceptibility Map: A Case Study Of TetouanMazari, Morocco. In MATEC Web of Conferences (Vol. 149, p. 02082).EDP Sciences
5. Bui DT, Tuan TA, Klempe H, Pradhan B, Revhaug I (2016) Spatial prediction models for shallow landslide hazards: a comparative assessment of the efficacy of support vector machines, artificial neural networks, kernel logistic regression, and logistic model tree. Landslides 13(2):361–378
6. BUWAL B (1997) BRP: Berücksichtigung der MassenbewegungsgefahrenbeiraumwirksamenTätigkeiten.Bundesamtfür Umwelt, Wald und Landschaft. BundesamtfürWasserwirtschaft, BundesamtfürRaumplanung, Bern und Biel
7. Chalouan A, Michard A, El Kadiri K, Negro F, De Lamotte DF, Soto JI, Saddiqi O (2008) The Rif Belt. In: Continental evolution: the geology of Morocco. Springer, Berlin, pp 203–302
8. Crozier MJ (1984) Field assessment of slope instability. Slope instability, 103–142
9. Dai F, Lee CF (2002) Landslides on natural terrain. MT RES DEV 22(1):40–47
10. Devkota KC, Regmi AD, Pourghasemi HR, Yoshida K, Pradhan B, Ryu IC, Althuwaynee OF (2013) Landslide susceptibility mapping using certainty factor, index of entropy and logistic regression models in GIS and their comparison at Mugling–Narayanghat road section in Nepal Himalaya. Nat hazards 65(1):135–165
11. DURAND D (1980) La Méditerranée occidentale: étape de sa genèse et problèmes structuraux liés à celle-ci. Mem Soc Geol France 10:203–224
12. El Gharbaoui A (1980) La terre et l'homme dans la péninsule Tingitane. Test on the man and the natural environment in Rif Western. Dr Univ of Paris-Est Créteil Val de Marne, French
13. El Gharbaoui A (1987) Les climats: Géographie physique et géologie. Grande encyclopidie du Maroc, vol 3, p : 14-31
14. EL Kadiri K (1991) La Dorsale calcaire (Rif interne, Maroc): stratigraphie, sédimentologie et évolution géodynamique d'une marge alpine durant le Mésozoïque. Mise en évidence d'un modèle. Thèse Doct. Etat ès-Science, Univ. Abdelmalek Essaadi, Tétouan, 384p
15. El Kharim Y (2002) Etude des mouvements de versants dans la région de Tétouan (Rif occidental): Inventaire, analyse et cartographie. These Dr es SciUniv Abdelmalek Essaadi, Tétouan
16. EL Moutchou B (2014) Caractérisation morphosédimentaire, morphodynamique, géomorphologique et dynamique des versants du littoral méditerranéen marocain entre Fnideq et KaaAsresse (Provinces

de Tétouan et Chefchaouen, Maroc Nord Occidental). Thèse d'état. UAE, Tétouan.Tétouan.305 p

17. Elmoulat M, Ait Brahim L (2018) Landslides susceptibility mapping using GIS and weights of evidence model in Tetouan-Ras-Mazari area (Northern Morocco). Geomat Nat Haz Risk 9(1):1306–1325
18. Ercanoglu M, Gokceoglu C (2002) Assessment of landslide susceptibility for a landslide-prone area (north of Yenice, NW Turkey) by fuzzy approach. EnvGeol 41(6):720–730
19. Es-smairi A, El Moutchou B, Touhami AEO (2021) Landslide susceptibility assessment using analytic hierarchy process and weight of evidence methods in parts of the Rif chain (northernmost Morocco). Arab J Geosci 14:1346. https://doi.org/10.1007/s12517-021-07660-9
20. Fares A (1994) Essai méthodologique de la cartographie des risques naturels lies aux mouvements de terrain application a l'aménagement de la ville de Taounate. Rif, Maroc), Dr Diss, Besançon
21. Flageollet JC (1989) Les mouvements de terrains et leur prévention. (éd.) Masson, sérieGéographie, Paris, 224 p
22. Ghorbanzadeh O, Blaschke T, Gholamnia K, Meena SR, Tiede D, Aryal J (2019) Evaluation of different machine learning methods and deep-learning convolutional neural networks for landslide detection. Remote Sens-Basel 11(2):196
23. Glade T, Crozier MJ (2005) Landslide hazard and risk: concluding comment and perspectives. Landslide hazard and risk. Wiley, Chichester, pp 767–774
24. Goetz JN, Guthrie RH, Brenning A (2011) Integrating physical and empirical landslide susceptibility models using generalized additive models. Geomorphology 129(3-4):376–386
25. Guzzetti F (2006) Landslide Hazard and Risk Assessment. Mathematisch-NaturwissenschaftlichenFakultät der Rheinischen Friedrich-Wilhelms-Universität, University of Bonn Germany (Doctoral dissertation, Ph. D. Thesis)
26. Guzzetti F, Carrara A, Cardinali M, Reichenbach P, Galli M, Ardizzone F (1999) Landslide hazard evaluation: an aid to a sustainable development. Geomorphology 31(1-4):181–216
27. Hadji R, Limani Y, Baghem M, Demdoum A (2013) Geologic, topographic and climatic controls in landslide hazard assessment using GIS modeling: a case study of Souk Ahras region, NE Algeria. QuaternInt, 302, 224-237
28. Hamed Y, Ahmadi R, Hadji R, Mokadem N, Dhia HB, Ali W (2014) Groundwater evolution of the Continental Intercalaire aquifer of Southern Tunisia and a part of Southern Algeria: use of geochemical and isotopic indicators. Desalin Water Treat 52(10-12):1990–1996
29. He Q, Xu Z, Li S, Li R, Zhang S, Wang N, Chen W (2019) Novel entropy and rotation forest-based credal decision tree classifier for landslide susceptibility modeling. Entropy 21(2):106
30. Hong H, Tsangaratos P, Ilia I, Liu J, Zhu AX, Chen W (2018) Application of fuzzy weight of evidence and data mining techniques in construction of flood susceptibility map of Poyang County, China. Sci Total Environ 625:575–588

31. Iqbal J, Cui PENG, Hussain ML, Pourghasemi HR, Cheng DQ, Shah SU, Pradhan B (2021) Landslide Suscptibilty Assessment Along The Dubair-Dudishal Section Of The Karakoram Higway, Northwesternhimalayas, Pakistan. ActaGeodyn.Geomater., Vol. 18, No. 2 (202), 137–155, 2021
32. Jaafari A, Panahi M, Pham BT, Shahabi H, Bui DT, Rezaie F, Lee S (2019) Meta optimization of an adaptive neuro-fuzzy inference system with grey wolf optimizer and biogeography-based optimization algorithms for spatial prediction of landslide susceptibility. Catena 175:430–445
33. Kannan M, Saranathan E, Anabalagan R (2013) Landslide vulnerability mapping using frequency ratio model: a geospatial approach in Bodi-BodimettuGhat section, Theni district, Tamil Nadu. IndiaArab J Geosci 6(8):2901–2913
34. Karim Z, HadjiRHamed Y (2019) GIS-based approaches for the landslide susceptibility prediction in Setif Region (NE Algeria). GeotechGeolEng 37(1):359–374
35. Khosravi K, Pourghasemi HR, Chapi K, Bahri M (2016) Flash flood susceptibility analysis and its mapping using different bivariate models in Iran: a comparison between Shannon's entropy, statistical index, and weighting factor models. Environ Monit Assess 188(12):656
36. Lee S, Pradhan B (2007) Landslide Hazard Mapping at Selangor, Malaysia Using Frequency Ratio and Logistic Regression Models. Landslides 4:33–41. doi.org/10.1007/s10346-006-0047-y
37. Lee S, Talib JA (2005) Probabilistic landslide susceptibility and factor effect analysis. EnvGeol 47(7):982–990
38. Li X, Cheng X, Chen W, Chen G, Liu S (2015) Identification of forested landslides using LiDar data, object-based image analysis, and machine learning algorithms. Remote Sens 7(8):9705–9726
39. MATE/METL (1999) Plans de Prévention des Risques Naturels (PPR). In: Risques de Mouvements de Terrain, Ministère de l'Aménagement du Territoire et de l'Environnement, (MATE), Ministère de l'Equipement, des Transports et du Logement (METL). La Documentation Française, Paris
40. Millies-Lacroix A (1965) L'instabilité des versants dans le domaine rifain. GDYAC 15(7-8-9):97–109
41. Nohani E, Moharrami M, Sharafi S, Khosravi K, Pradhan B, Pham BT, Melesse M A (2019) Landslide susceptibility mapping using different GIS-based bivariate models. Water-Sui 11(7):1402
42. Park S, Choi C, Kim B, Kim J (2013) Landslide susceptibility mapping using frequency ratio, analytic hierarchy process, logistic regression, and artificial neural network methods at the Inje area. Korea Environ EartSci 68(5):1443–1464
43. Pham BT, Bui DT, Prakash I (2018) Application of classification and regression trees for spatial prediction of rainfall-induced shallow landslides in the Uttarakhand area (India) using GIS. In: Climate change, extreme events and disaster risk reduction. Springer, Cham, pp 159–170
44. Popesc ME (1994) A suggested method for reporting landslide causes. Geol B AssocIntGeolIng 50(1):71–74
45. Pourghasemi HR, Mohammady M, Pradhan B (2012b) Landslide susceptibility mapping using index of entropy and conditional probability models in GIS: Safarood Basin, Iran. Catena 97:71–84

46. Pourghasemi HR, Moradi HR, Aghda SF (2013) Landslide susceptibility mapping by binary logistic regression, analytical hierarchy process, and statistical index models and assessment of their performances. Nat Hazards 69(1):749–779
47. Pourghasemi HR, Pradhan B, Gokceoglu C (2012a) Application of fuzzy logic and analytical hierarchy process (AHP) to landslide susceptibility mapping at Haraz watershed, Iran. Nat Hazard 63(2):965–996
48. Pradhan B (2010) Landslide susceptibility mapping of a catchment area using frequency ratio, fuzzy logic and multivariate logistic regression approaches. J Indian Soc Remote Sens 38(2):301–320
49. Pradhan B (2011) Manifestation of an advanced fuzzy logic model coupled with geo-information techniques to landslide susceptibility mapping and their comparison with logistic regression modelling. Environ Ecol Stat 18(3):471–493
50. Pradhan B (2013) A comparative study on the predictive ability of the decision tree, support vector machine and neuro-fuzzy models in landslide susceptibility mapping using GIS. ComputGeosci 51(1):350–365
51. Pradhan B, Lee S (2010a) Regional landslide susceptibility analysis using back-propagation neural networks model at Cameron Highland. Malaysia Landslides 7(1):13–30
52. Pradhan B, Lee S (2010b) Delineation of landslide hazard areas on Penang Island, Malaysia, by using frequency ratio, logistic regression, and artificial neural network models. Environ Earth Sci 60(5):1037–1054
53. Pradhan B, Lee S, Buchroithner MF (2010b) A GIS-based back-propagation neural network model and its cross-application and validation for landslide susceptibility analyses. Comput Environ Urban Syst 34(3):216–235
54. Pradhan B, Oh HJ, Buchroithner M (2010a) Weights-of-evidence model applied to landslide susceptibility mapping in a tropical hilly area. Geomat Nat Haz Risk 1(3):199–223
55. Rasyid AR, Bhandary NP, Yatabe R (2016) Performance of frequency ratio and logistic regression model in creating GIS based landslides susceptibility map at Lompobattang Mountain, Indonesia. Geo environ Disasters 3(1):19
56. Regmi AD, Devkota KC, Yoshida K, Pradhan B, Pourghasemi HR, KumamotoT, Akgun A (2014) Application of frequency ratio, statistical index, and weights-of-evidence models and their comparison in landslide susceptibility mapping in Central Nepal Himalaya. Arab J Geosci 7(2):725–742
57. Regmi NR, GiardinoJR,Vite JD (2010) Modeling susceptibility to landslides using the weight of evidence approach: Western Colorado, USA. Geomorphology 115(1-2):172–187
58. Saadatkhah N, Kassim A, Lee LM (2015) Susceptibility assessment of shallow landslides in Hulu Kelang area, Kuala Lumpur, Malaysia using analytical hierarchy process and frequency ratio. Geotech Geol Eng 33(1):43–57
59. Sadisun IA, Arifianti Y (2018) Weights of evidence method for landslide susceptibility mapping in Takengon, Central Aceh, Indonesia. IOP Conf. Ser. Earth Environ Sci (Vol 118(1):012037

60. Saha S, Saha A, Hembram TK, Pradhan B, Alamri AM (2020) Evaluating the performance of individual and novel ensemble of machine learning and statistical models for landslide susceptibility assessment at Rudraprayag District of Garhwal Himalaya. App Sci 10(11):3772
61. Song KY, Oh HJ, Choi J, Park I, Lee C, Lee S (2012) Prediction of landslides using ASTER imagery and data mining models. AdvSpaceRes 49(5):978–993
62. Suter G (1980) Carte géologique et structurale de la chaîne Rifaine au 1/500.000. Notes etMém. Serv. géol.,Maroc, p 245
63. Thapa D, Bhandari BP (2019) GIS-Based Frequency Ratio Method for Identification of Potential Landslide Susceptible Area in the Siwalik Zone of Chatara-Barahakshetra Section. NepalOpen J of Geol 9(12):873
64. Thauvin JP (1971) Ressources en eau du Maroc. Notes et mém, ser, géol, Maroc, T. 1, N°. 231 p:113 123
65. Thiery Y, Malet JP, Sterlacchini S, Puissant A, Maquaire O (2007) Landslidesusceptibilityassessment by bivariatemethods at large scales: application to a complexmountainousenvironment. Geomorphology 92(1-2):38–59
66. Trigila A, Iadanza C, Esposito C, Scarascia-Mugnozza G (2015) Comparison of Logistic Regression and Random Forests techniques for shallow landslide susceptibility assessment in Giampilieri (NE Sicily, Italy). Geomorphology 249:119–136
67. Van Den Eeckhaut M, Kerle N, Poesen J, Hervás J (2012) Object-oriented identification of forested landslides with derivatives of single pulse LiDAR data. Geomorphology 173:30–42
68. Van Westen CJ (2000) The modelling of landslide hazards using GIS. SurvGeophys 21(2-3):241–255
69. Van Westen CJ, Van Asch TW, Soeters R (2006) Landslide hazard and risk zonation—why is it still so difficult? B Enggeol Environ 65(2):167–184
70. Varnes DJ (1978) Slope movement types and processes. In: Schuster RL, Krizek RJ (eds) “Landslides: Analysis and control”. Natl AcadSci, Washington
71. Vijith H, Krishnakumar KN, Pradeep GS, Ninu Krishnan MV, Madhu G (2014) Shallow landslide initiation susceptibility mapping by GIS-based weights-of-evidence analysis of multi-class spatial data-sets: a case study from the natural sloping terrain of Western Ghats, India. Georisk: Assessment and Management of Risk for Engineered Systems and Geohazards, 8(1), pp 48–62
72. Wan S (2009) A spatial decision support system for extracting the core factors and thresholds for landslide susceptibility map. Eng Geol 108(3-4):237–251
73. Wildi W (1983) La chaîne tello-rifaine (Algérie, Maroc, Tunisie): structure, stratigraphie et évolution du Trias au Miocène. Rev Geogr Phys Geol 24(3):201–297
74. Wu Z, Wu Y, Yang Y, Chen F, Zhang N, Ke Y, Li W (2017) A comparative study on the landslide susceptibility mapping using logistic regression and statistical index models. Arab J Geosci 10(8):187

75. Yalcin A, Reis S, Aydinoglu AC, Yomralioglu T (2011) A GIS-based comparative study of frequency ratio, analytical hierarchy process, bivariate statistics and logistics regression methods for landslide susceptibility mapping in Trabzon. NE Turkey Catena 85(3):274–287
76. Yilmaz I (2010) Comparison of landslide susceptibility mapping methodologies for Koyulhisar, Turkey: conditional probability, logistic regression, artificial neural networks, and support vector machine. Earth Environ Sci 61(4):821–836
77. Yilmaz I (2009) Landslide Susceptibility Mapping Using Frequency Ratio, Logistic Regression, Artificial Neural Networks and Their Comparison: A Case Study from Kat Landslides (Tokat-Turkey).ComputGeosci, 35, 1125–1138
78. Zhang W, Goh AT, Zhang Y, Chen Y, Xiao Y (2015) Assessment of soil liquefaction based on capacity energy concept and multivariate adaptive regression splines. EngGeol 188:29–37
79. Zorn M, Komac B (2007) Probability modelling of landslide hazard.ActaGeogrSlov 47(2), 139–169

Tables

Table.1. Indices of multi-collinearity diagnosis for landslide triggers factors of the study area.

Model	Collinearity statistics	
	Tolerance	VIF
Land use	0,904	1,106
Lithology	0,391	2,557
Aspect	0,991	1,009
Stream	0,971	1,03
Rainfall	0,832	1,201
Shaded	0,969	1,032
Altitude	0,195	5,141
Slop	0,220	4,552
Curvature	0,983	1,017
Fault	0,712	1,404
Road	0,903	1,108

Table.2: Correlation between landslides occurrence and each conditioning factor using FR and SE models.

Factor	*Factor Class*	*Numbers of Pixels*	*Percent of Pixels*	*Landslide Numbers*	*Percent of Landslide*	*FR*	*SE*
Elevation (m)	<25	201643	10,690	1575	1,660	0,155	
	25 - 100	264516	14,023	12245	12,905	0,920	
	100 - 600	954718	50,614	60171	63,415	1,253	0,200
	>600	465400	24,673	20894	22,020	0,892	
Slope (°)	<2.5	164427	8,717	1284	1,353	0,155	
	2.5 - 5	127393	6,754	3401	3,584	0,531	
	5 - 15	558690	29,619	38018	40,067	1,353	0,175
	15- 20	332397	17,622	18557	19,557	1,110	
	>20	703370	37,289	33625	35,438	0,950	
Aspect	N	518452	27,485	29648	31,246	1,137	
	E	519854	27,560	26260	27,676	1,004	0,016
	S	399591	21,184	14690	15,482	0,731	
	O	448380	23,771	24287	25,596	1,077	
Curvature	Concave	872423	46,251	48319	50,924	1,101	
	Flat	149588	7,930	7433	7,834	0,988	0,005
	Convex	864266	45,819	39133	41,243	0,900	
Hill shade/relief (m)	0-50	24882	1,319	843	0,888	0,674	
	50-100	120178	6,371	4324	4,557	0,715	
	100-150	369378	19,582	17272	18,203	0,930	0,028
	150-200	908220	48,149	42994	45,312	0,941	
	200-254	463619	24,579	29452	31,040	1,263	
Proximity to Streams (m)	<30	376524	19,961	24507	25,828	1,294	
	30-60	335536	17,788	21010	22,143	1,245	
	60-90	297363	15,765	16960	17,874	1,134	
	90-120	255113	13,525	12606	13,286	0,982	
	90-150	208257	11,041	8617	9,082	0,823	

	150-180	155961	8,268	5257	5,540	0,670	0,074
	180-210	109286	5,794	2930	3,088	0,533	
	210-240	71085	3,769	1594	1,680	0,446	
	240-270	41651	2,208	787	0,829	0,376	
	>270	35501	1,882	617	0,650	0,346	
Proximity to Faults(m)	<30	75920	4,025	1258	1,326	0,329	0,053
	30-60	74365	3,942	2492	2,626	0,666	
	60-90	71041	3,766	3611	3,806	1,010	
	90-120	67641	3,586	4279	4,510	1,258	
	120-150	64601	3,425	4542	4,787	1,398	
	150-180	60951	3,231	4589	4,836	1,497	
	180-210	57478	3,047	4318	4,551	1,493	
	210-300	153926	8,160	11568	12,192	1,494	
	300-500	256283	13,587	18236	19,219	1,415	
	>500	1004071	53,230	39992	42,148	0,792	
Proximity to Roads (m)	<40	65808	3,489	2594	2,734	0,784	0,004
	40-80	46208	2,450	1816	1,914	0,781	
	80-120	43611	2,312	1827	1,925	0,833	
	120-160	41418	2,196	1659	1,748	0,796	
	160-200	39292	2,083	1682	1,773	0,851	
	200-240	37340	1,980	1731	1,824	0,922	
	240-280	35663	1,891	1760	1,855	0,981	
	280-320	33739	1,789	1711	1,803	1,008	
	320-360	32434	1,719	1602	1,688	0,982	
	>360	1510764	80,092	78503	82,735	1,033	
Land-use/Cover	Water Bodies	16270	0,863	223	0,235	0,272	0,065
	barren land	1158850	61,436	63771	67,209	1,094	
	Shurbland and Sparsely vegetated	53609	2,842	1756	1,851	0,651	

	Agriculture land	61195	3,244	2779	2,929	0,903	
	Settlement area	31073	1,647	1458	1,537	0,933	
	Wood and forest	565280	29,968	24898	26,240	0,876	
Lithology	Gneiss and Micaschists	156561	8,300	4987	5,256	0,633	
	Peridotites and Kinzigites	55225	2,928	749	0,789	0,270	
	Shale complex	417931	22,156	19560	20,614	0,930	
	marlstones	41020	2,175	1936	2,040	0,938	
	Dolomite	181724	9,634	9952	10,488	1,089	0,141
	Limestone	146268	7,754	8056	8,490	1,095	
	Sandstone-Pelite	299362	15,871	27121	28,583	1,801	
	Conglomerates	61635	3,268	3990	4,205	1,287	
	Sandstones - marlstones	19406	1,029	2796	2,947	2,864	
	Marlstones-Limestone	43379	2,300	5492	5,788	2,517	
	Limestone-dolomite	123641	6,555	7562	7,970	1,216	
	Alluvium	340125	18,032	2684	2,829	0,157	
Rainfall (mm/year)	<500	0	0,000	0	0,000	0,000	
	500-550	104	0,006	0	0,000	0,000	
	550-600	26524	1,406	661	0,697	0,495	
	600-650	144742	7,673	6644	7,002	0,913	
	650-700	789042	41,831	37855	39,896	0,954	
	700-750	691076	36,637	36686	38,664	1,055	0,238
	750-800	161945	8,585	10788	11,370	1,324	
	800-850	35891	1,903	1594	1,680	0,883	
	850-900	14564	0,772	359	0,378	0,490	
	>900	22389	1,187	298	0,314	0,265	

Figures

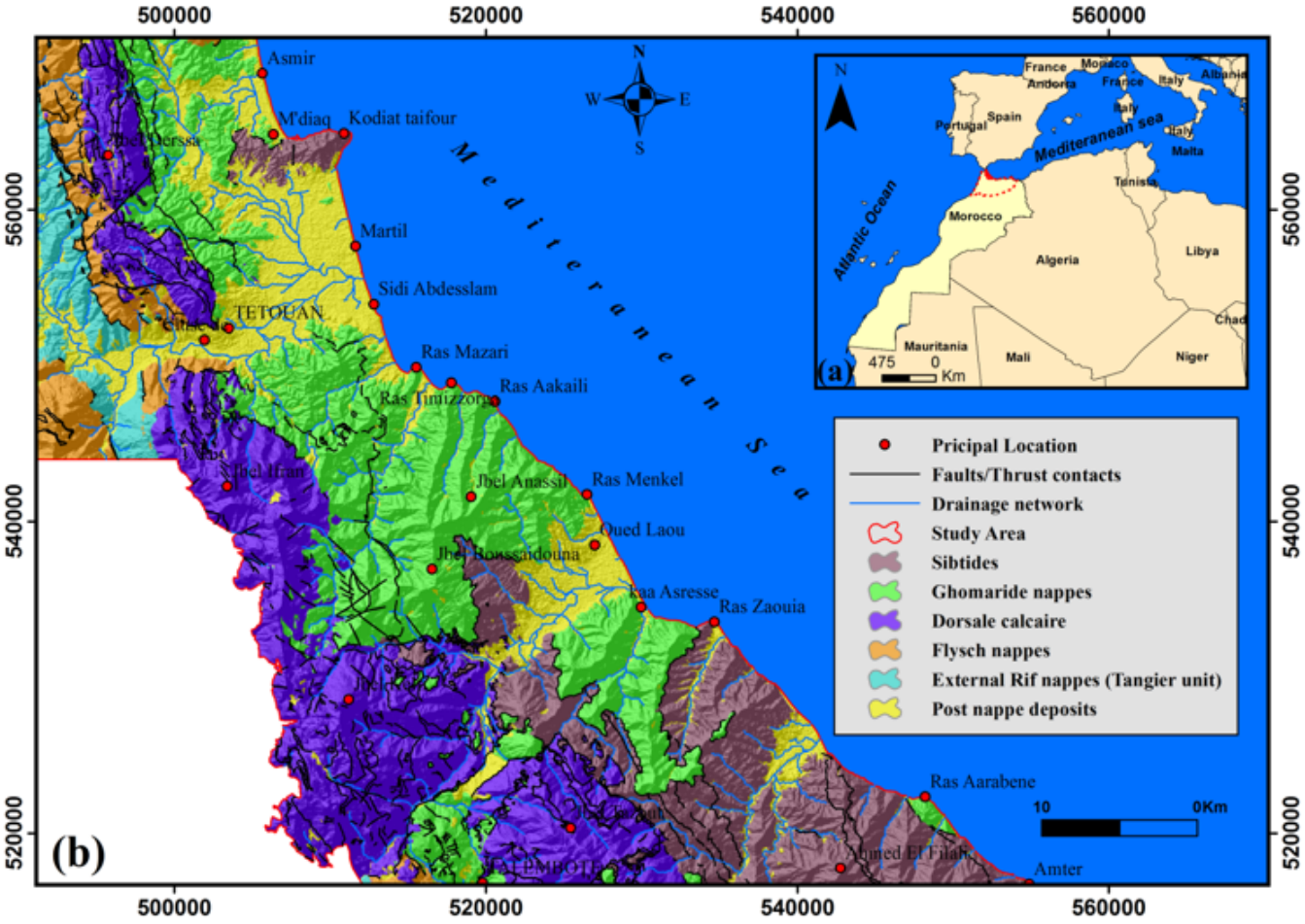

Figure 1

Location of the study area at (**a)** national scale (**b)** Structural schema of the study area (modified after, Es-smairi et al.2021,)

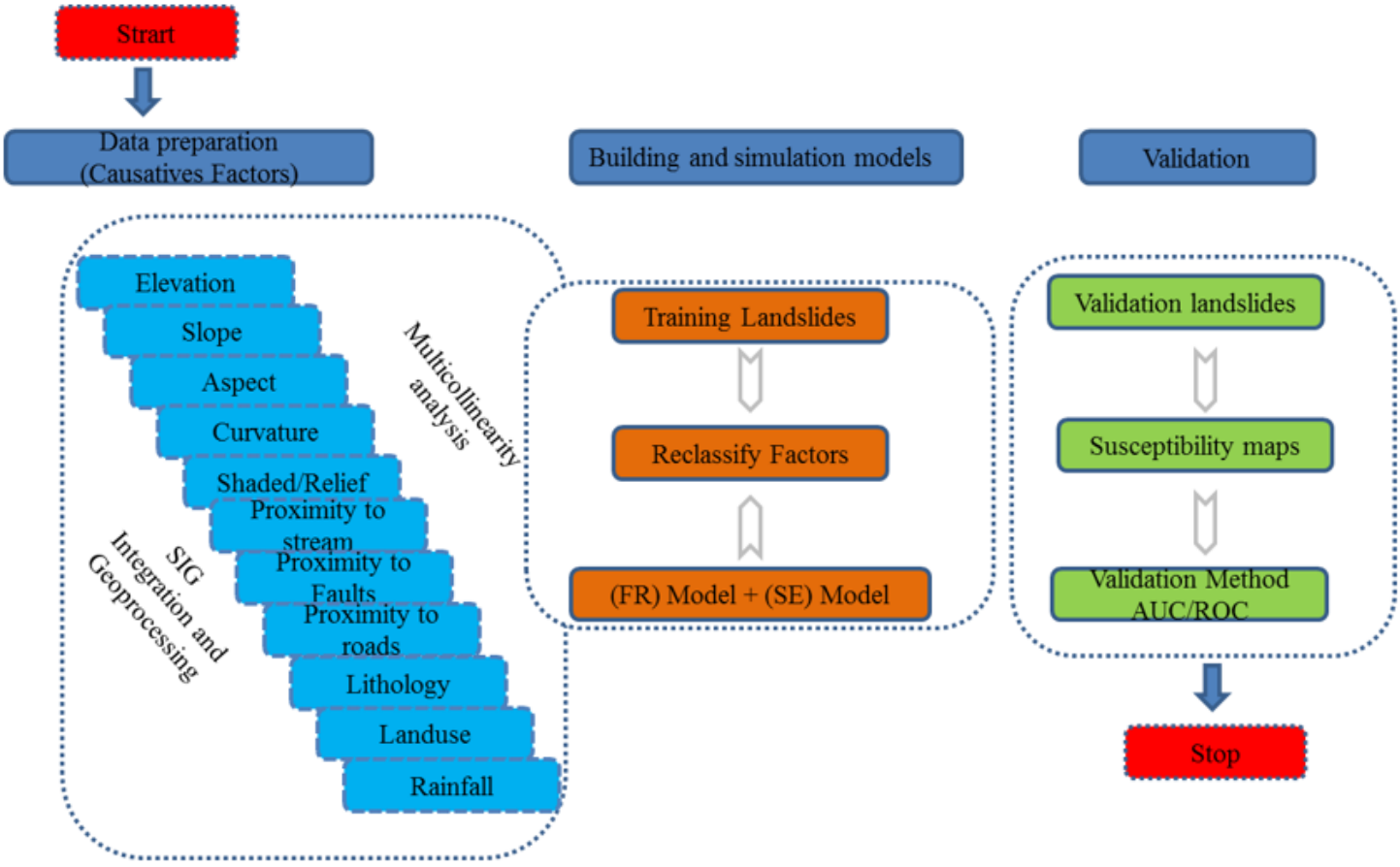

Figure 2

Flowchart of the methodology followed in this study

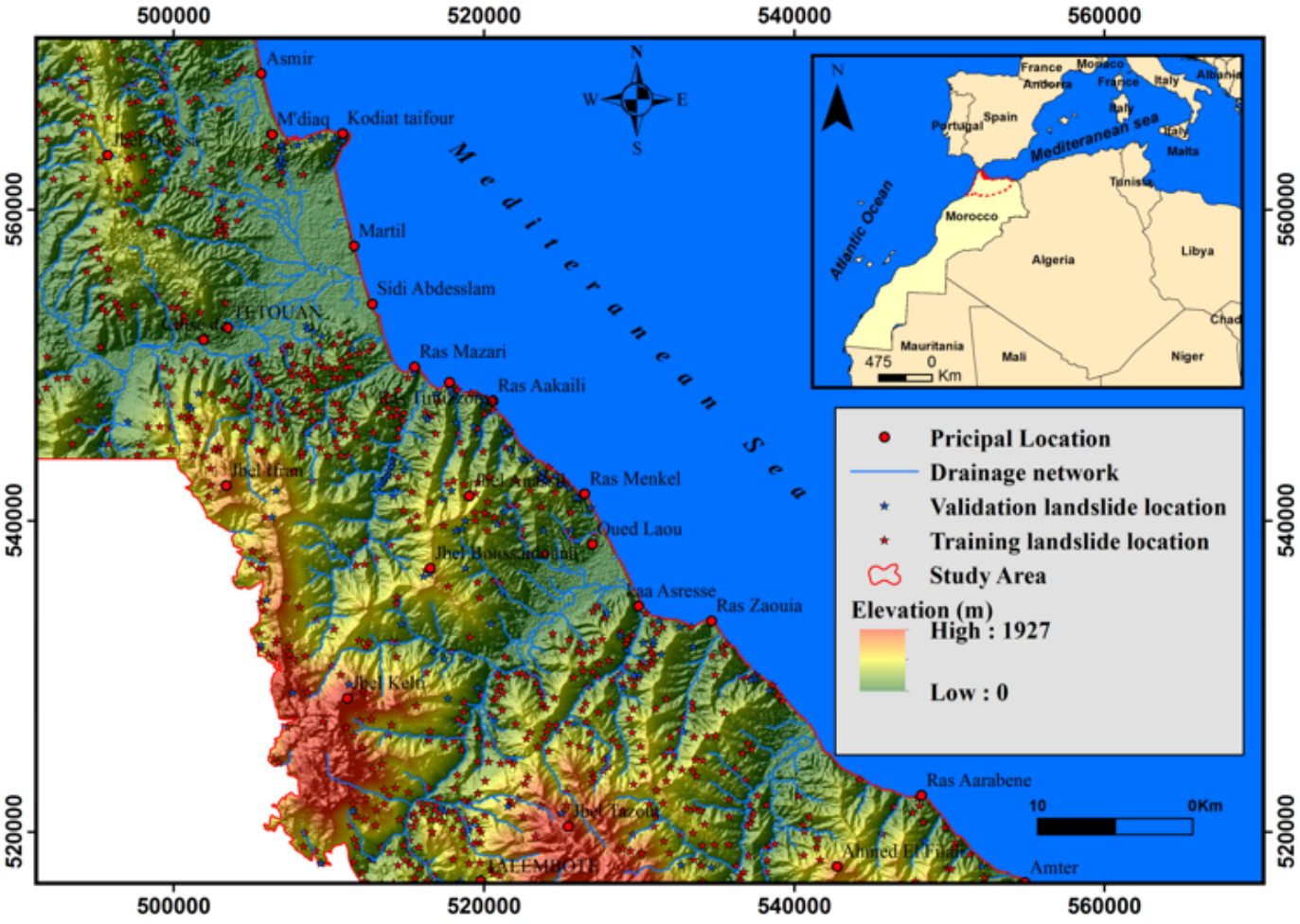

Figure 3

Location of inventoried landslides and its distribution in the study area.

Figure 4

Field photographs of landslides types observed in the study area.

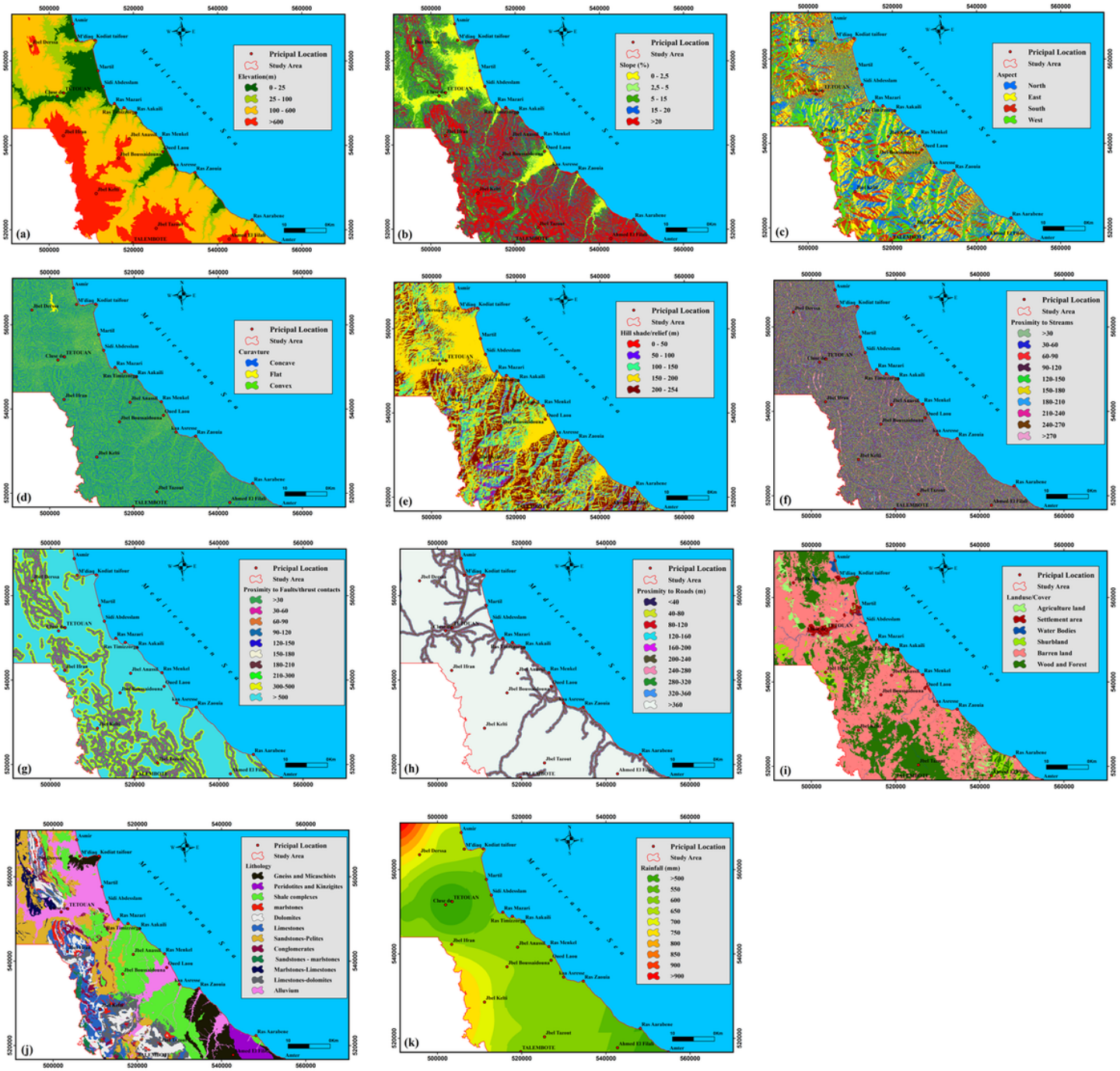

Figure 5

Thematic maps of (a) Elevation, (b) Slope (c) Aspect (d) Curvature (e) Shaded/relief (f) Proximity to stream (g) Proximity to faults (h) Proximity to roads (i) Land use (j) Lithology (k) rainfall (mm).

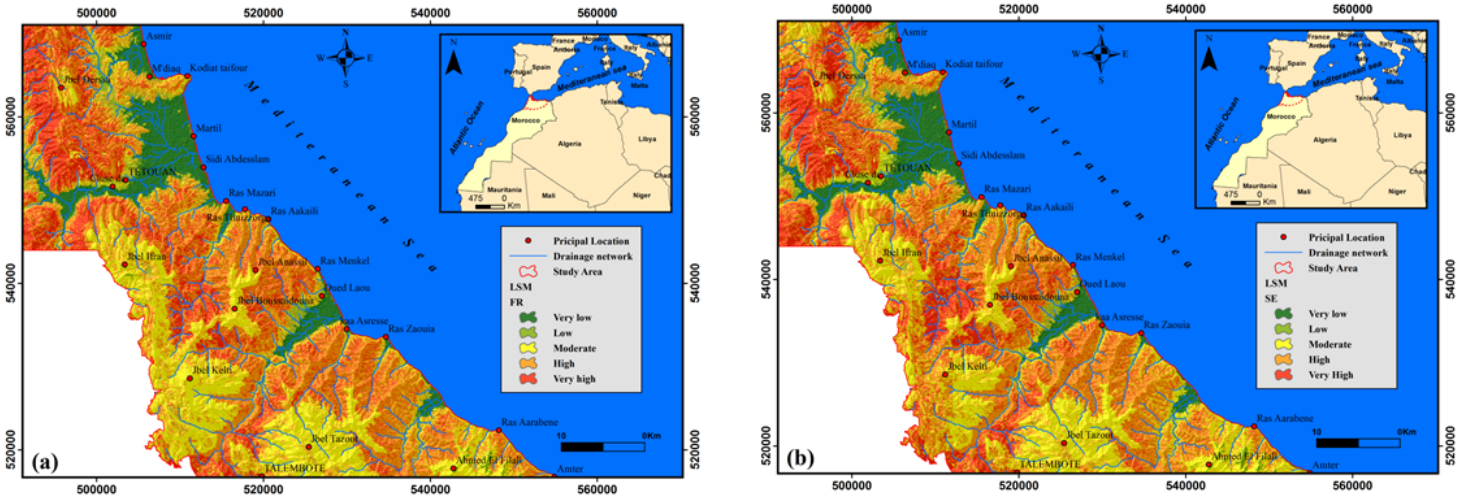

Figure 6

Landslide susceptibility maps prepared by using (a) FR model and (b) SE model of the study area.

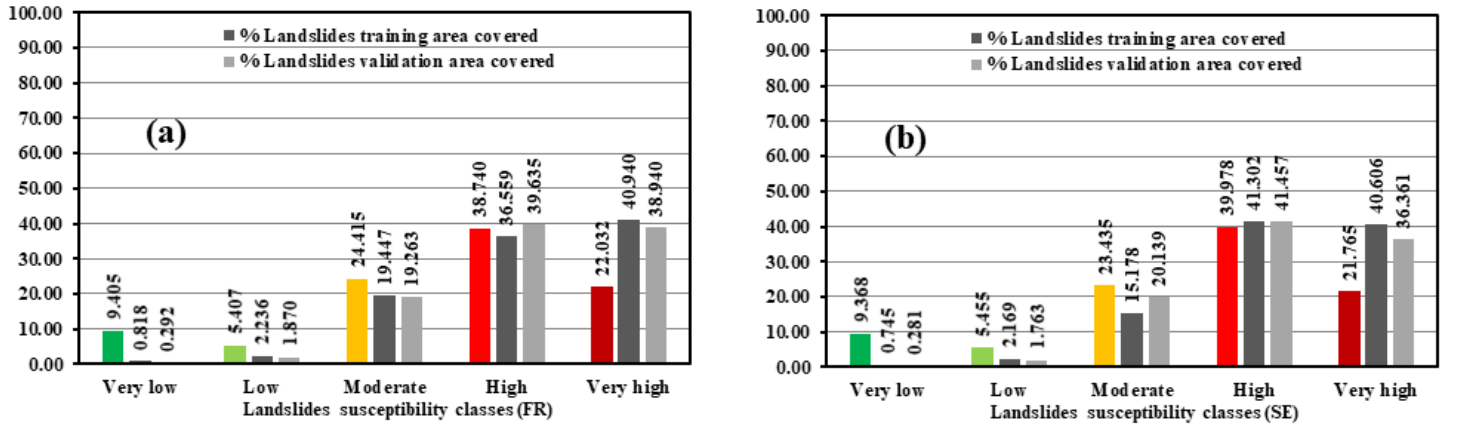

Figure 7

Percentage of landslide susceptibility classes and landslides inventory on landslides susceptibility maps (Training and validation data) for (a) FR model and (b) SE model.

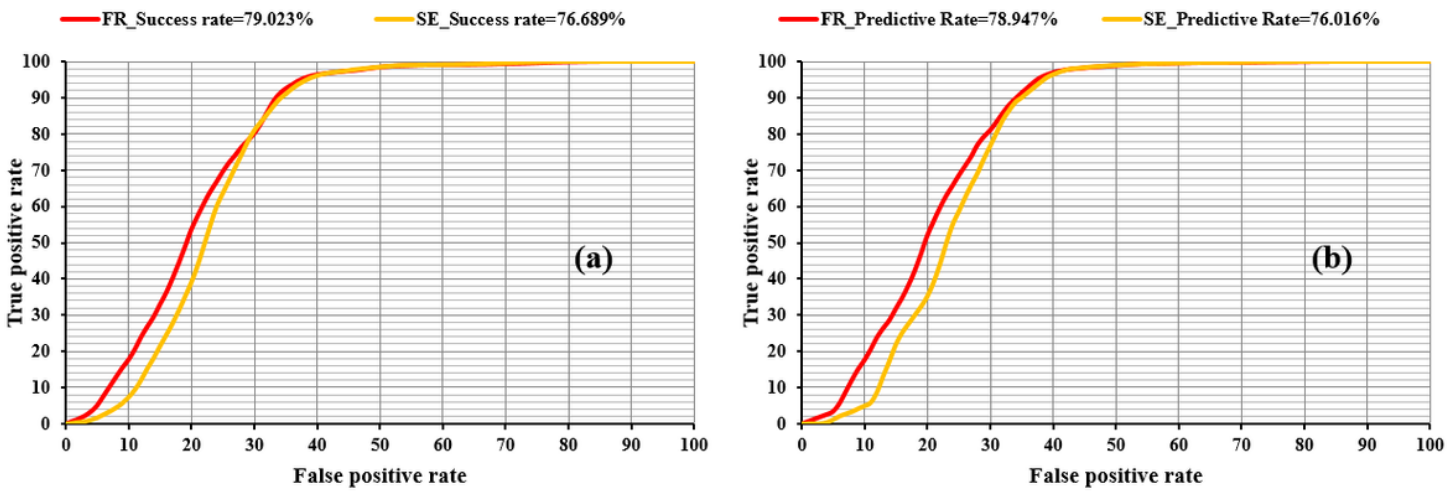

Figure 8

Success rate curve and the predictive rate of landslides susceptibility index map, for (a) FR and (b) SE model in the study area.